

Lattice-Boltzmann Simulations of Fluid Flows in MEMS

Xiaobo Nie¹, Gary D. Doolen¹ and Shiyi Chen^{1,2}

¹Center for Nonlinear Studies and Theoretical Division, Los Alamos National Laboratory, Los Alamos, NM 87545

²IBM Research Division, T. J. Watson Research Center, P.O. Box 218, Yorktown Heights, NY 10598

The lattice Boltzmann model is a simplified kinetic method based on the particle distribution function. We use this method to simulate problems in MEMS, in which the velocity slip near the wall plays an important role. It is demonstrated that the lattice Boltzmann method can capture the fundamental behavior in micro-channel flow, including velocity slip and nonlinear pressure drop along the channel. The Knudsen number dependence of the position of the vortex center and the pressure contour in micro-cavity flows is also demonstrated.

The development of technologies in Micro-electro-mechanical systems (MEMS) has motivated the study of fluid flows in devices with micro-scale geometries, such as micro-channel and micro-cavity flows [1]. In these flows, the molecular mean free path of fluid molecules could be the same order as the typical geometric length of the device; then the continuum hypothesis which is the fundamental for the Navier-Stokes equation breaks down. An important feature in these flows is the emergence of a slip velocity at the flow boundary, which strongly affects the mass and heat transfer in the system. In micro-channel experiments, it has been observed that the measured mass flow rate is higher than that based on a non-slip boundary condition [2]. The Knudsen number, $K_n = l/L$, can be used to identify the influence of the effects of the mean free path on these flows, where l is the mean free path of molecules and L is the typical length of the flow domain. It has been pointed out that for a system with $K_n < 0.001$, the fluid flow can be treated as continuum. For $K_n > 10$ the system can be considered as a free-molecular flow. The fluid flow for $0.001 < K_n < 10$, which often appears in the MEMS [1], can not be considered as a continuum nor a free-molecular flow. Traditional kinetic methods, such as molecular dynamics simulations [3] and the continuum Boltzmann equation approach, could be used to describe these flows. But these methods are more complicated than schemes usually used for continuum hydrodynamic equations. The solution of the Navier-Stokes equation including the velocity-slip boundary condition with a variable parameter has also been used to simulate micro-channel flows [4].

In the past ten years, the lattice Boltzmann method (LBM) [5] has emerged as an alternative numerical technique for simulating fluid flows. This method solves a simplified Boltzmann equation on a discretized lattice. The solution of the lattice Boltzmann equation converges to the Navier-Stokes solution in the continuum limit (small Knudsen number). In addition, since the lattice Boltzmann method is intrinsically kinetic, it can be also used to simulate fluid flows with high Knudsen numbers, including fluid flows in very small MEMS.

To demonstrate the utility of the LBM, we use the LBM model with three speeds and nine velocities on a two-dimensional square lattice. The velocities, \mathbf{c}_i , include eight moving velocities along the links of the square

lattice and a zero velocity for the rest particle. They are: $(\pm 1, 0)$, $(0, \pm 1)$, $(\pm 1, \pm 1)$, $(0, 0)$. Let $f_i(\mathbf{x}, t)$ be the distribution functions at \mathbf{x} , t with velocity \mathbf{c}_i . The lattice Boltzmann equation with the BGK collision approximation [6,7] can be written as

$$f_i(\mathbf{x} + \mathbf{c}_i \delta x, t + \delta t) - f_i(\mathbf{x}, t) = -\tau^{-1}(f_i - f_i^{eq}), \quad (1)$$

where f_i^{eq} ($i = 0, 1, \dots, 8$) is the equilibrium distribution function and τ is the relaxation time. We have assumed that the spatial separation of the lattice is δx and the time step is δt . A suitable equilibrium distribution is [7]:

$$f_i^{eq} = t_i \rho \left[1 + \frac{c_{i\alpha} u_\alpha}{c_s^2} + \frac{(c_{i\alpha} c_{i\beta} - c_s^2 \delta_{\alpha\beta}) u_\alpha u_\beta}{2c_s^4} \right]. \quad (2)$$

Here $c_s = 1/\sqrt{3}$, $t_0 = 4/9$, $t_1 = t_2 = t_3 = t_4 = 1/9$ and $t_5 = t_6 = t_7 = t_8 = 1/36$. The Greek subscripts α and β denote the spatial directions in Cartesian coordinates. The density ρ and the fluid velocity \mathbf{v} are defined by $\rho = \sum_i f_i$, $\rho \mathbf{v} = \sum_i \mathbf{c}_i f_i$. In previous lattice-BGK models, τ was chosen to be a constant. This is applicable only for nearly-incompressible fluids. In micro-flows, the local density variation is still relatively small, but the total density change, for instance the density difference between the inlet and exit of a very long channel, could be quite large. To include the dependence of viscosity on density we replace τ in Eq.(1) by τ' : $\tau' = \frac{1}{2} + \frac{1}{\rho}(\tau - \frac{1}{2})$. Using the Chapman-Enskog multi-scale expansion technique, we obtain the following Navier-Stokes equations in the limit of long wavelength and low Mach number:

$$\partial_t \rho + \partial_\alpha (\rho u_\alpha) = 0, \quad (3)$$

$$\partial_t (\rho u_\alpha) + \partial_\beta (\rho u_\alpha u_\beta) = -\partial_\alpha P - \partial_\beta \pi_{\alpha\beta}, \quad (4)$$

$$P = c_s^2 \rho, \quad \pi_{\alpha\beta} = \nu (\partial_\alpha (\rho u_\beta) + \partial_\beta (\rho u_\alpha)),$$

where $\nu = c_s^2(2\tau - 1)/(2\rho)$ is the kinematic viscosity. In classical kinetic theory, the viscosity ν for a hard sphere gas is linearly proportional to the mean free path. Similarly, we define the mean free path l in the LBM as: $a(\tau - 0.5)/\rho$, where a is constant.

Our first numerical example is a micro-channel flow [2]. The flow is contained between two parallel plates separated by a distance H and driven by the pressure difference between the inlet pressure, P_i , and exit pressure, P_e . The channel length in the longitudinal direction is L . We

take $L = 1000, H = 10$ (lattice units) in our simulations satisfying $L/H \gg 1$. The bounce-back boundary condition is used for the particle distribution functions at the top and bottom plates, i.e., when a particle distribution hits a wall node, the particle distribution scatters back to the fluid node opposite to its incoming direction. A pressure boundary condition is used at the input and the exit.

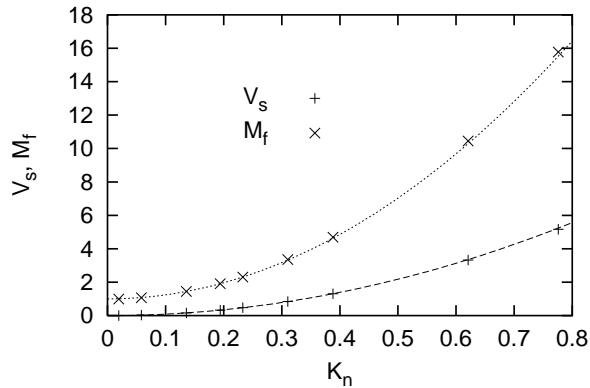


FIG. 1. The slip velocity and the normalized mass flow rate at the exit of a micro-channel flow as functions of K_n for $P_i/P_e = 2$. The '+' and 'x' are LBM numerical results. The dashed and dotted lines are Eq.(5) and Eq.(6) respectively.

The slip velocity V_s at the exit of the micro-channel flow is defined as: $u(y) = u_0(Y - Y^2 + V_s)$, where $u(y)$ is the velocity along the x (or flow) direction at the exit and $Y = y/H$. u_0 and V_s can be obtained by fitting numerical results using the least squares method. This definition of the slip velocity is consistent with others [2,4]. In Fig. 1, we plot the slip velocity V_s and the normalized mass flow rate $M_f = M/M_0$, as functions of Knudsen number when the pressure ratio $\eta = P_i/P_e = 2$. The normalization factor, $M_0 = \frac{h^3 P_e}{24\nu}(\eta - 1)$, is the mass flow rate when the velocity slip is zero. To calculate the Knudsen number we have chosen $a = 0.388$ in order to match the simulated mass flow rate with experiments (See theory curve in Fig. 3). Using a least squares fit to the data in Fig. 1, we obtain:

$$V_s = 8.7K_n^2. \quad (5)$$

If we assume that the Navier-Stokes equations are valid for the micro-flows except that the slip boundary condition V_s in Eq.(5) replaces the traditional non-slip condition on the walls [4], Eqs. (3), (4) and (5) will give the mass flow rate:

$$M_f = 1 + 12V_s(K_n) \frac{\ln(\eta)}{\eta^2 - 1}. \quad (6)$$

For $\eta = 2$, the above formula becomes $M_f = 1 + 24.1K_n^2$, which agrees well with the numerical results in Fig 1.

In laminar Poiseuille flows, one usually assumes that the density variation along the channel is very small, and the pressure drop along the channel is nearly linear. In

micro-channel flow, however, the ratio between the length and the width is much larger and the pressure drop is not linear. If there is no velocity slip at the walls, it has been shown [2,4] from the Navier-Stokes equation that the pressure along the channel has the following dependence on the dimensionless coordinate, $X = x/L$:

$$P^2 = P_e^2[1 + (\eta^2 - 1)(1 - X)], \quad (7)$$

If the velocity at the boundaries is allowed to slip, the pressure drop along the channel will depend on the Knudsen number. In Fig. 2 we present the LBM simulation results for the normalized pressure deviation from a linear pressure drop, $(P - P_l)/P_e$, as functions of X for several Knudsen numbers, where $P_l = P_e + (P_i - P_e)(1 - X)$. It is seen that when $K_n \leq 0.2$, $(P - P_l)/P_e$ is a positive nonlinear function of X . This agrees with the results in [4] using an engineering model. For $K_n \geq 0.2$, the LBM simulation shows that $(P - P_l)/P_e$ becomes negative, which is directly linked to the fact that the slip velocity depends on the square of K_n in the LBM. For large K_n , the pressure can be derived from Eq.(6):

$$P = P_e[\eta^{(1-X)}]. \quad (8)$$

The negative deviation from a linear pressure drop has not been experimentally observed before and it would be interesting to testify this experimentally.

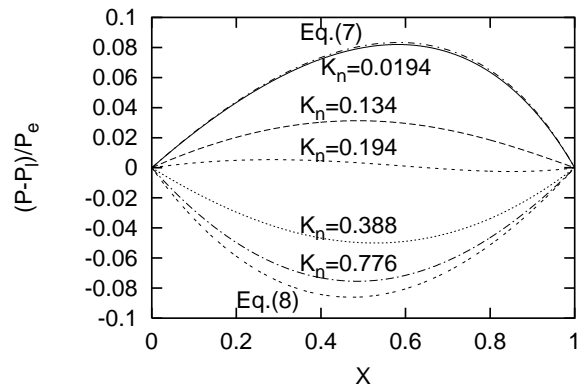


FIG. 2. The deviations from linear pressure drop for $\eta = P_i/P_e = 2$. The top and bottom lines are the analytical results from Eq.(7) for $K_n = 0$ and Eq.(8) for $K_n \gg 1$ respectively. The other curves are LBM numerical results for the Knudsen numbers indicated.

In Fig. 3 the mass flow rates as functions of the pressure ratio η when $K_n = 0.165$ are shown for our theory, the experimental work [2], the engineering model [4] and the LBM simulation. Our theory and the LBM simulation agree well with the experimental measurements. It is noted that for large pressure ratios ($\eta \geq 1.8$), the LBM agrees reasonably well with Beskok et al. [4]. But for smaller pressure ratios, the difference increases because of different dependence of the slip velocity on K_n .

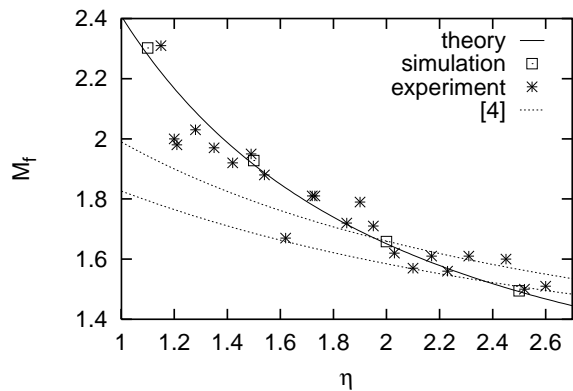


FIG. 3. The normalized mass flow rate as a function of the pressure ratio for $K_n = 0.165$. The theory is Eq.(6).

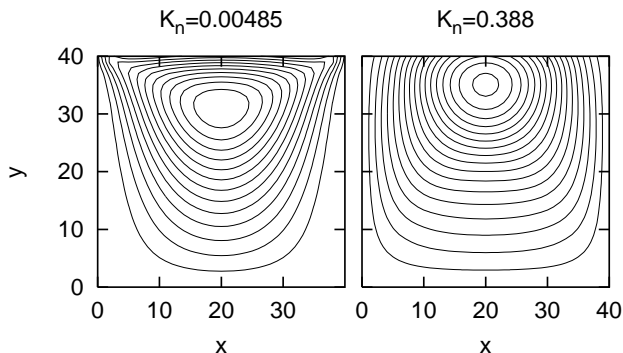


FIG. 4. Streamlines for two Knudsen numbers.

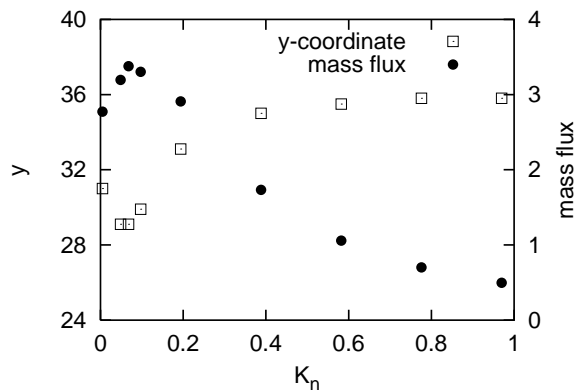


FIG. 5. The y -coordinate of the vortex center (square symbols) and the mass flux (solid circles) as a function of K_n .

Our second LBM numerical simulation is the two-dimensional micro-cavity flow. The cavity size is $L_x = L_y = 40$ (lattice units). The upper wall moves with a constant velocity, v_0 , from left to right. The other three walls are at rest, and bounce-back boundary conditions are used. To see the dependence on the Knudsen number in our simulations, we fixed the Reynolds number, $Re = \frac{v_0 L_x}{\nu} = 2.4 \times 10^{-4}$ and require the Mach number to be small, $Ma = \frac{v_0}{c_s} \leq 10^{-3}$. In Fig. 4, we show the streamlines for two different Knudsen numbers. In Fig. 5 we show the vertical positions of the vortex center and the mass flux between the bottom and the vortex cen-

ter as functions of K_n . It can be seen that the center moves upward and the mass flow decreases with increasing Knudsen number. This occurs because the slip velocity on the upper wall causes momentum transfer to be less efficient. It has been shown [8] that the center of the vortex moves downward when the Reynolds number increases for very small K_n . Fig. 6 shows the pressure contours for the same parameters as in Fig. 4. Totally different pressure structures are observed for these two cases. When the Knudsen number is small, the continuum assumption is valid and the pressure contours are almost circles with centers at the left or the right corners. On the other hand, due to the slip velocity on the walls, the pressure contours become nearly straight lines at the higher Knudsen number.

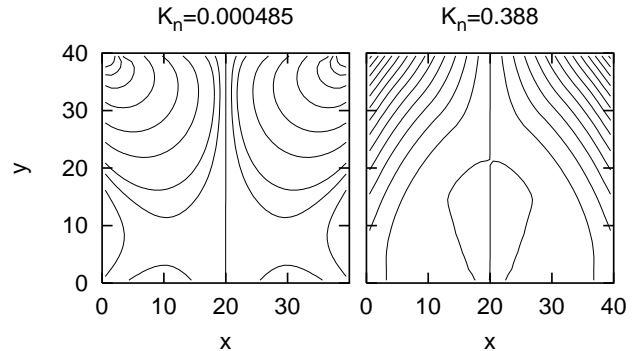


FIG. 6. The contours of pressure for the same two Knudsen numbers shown in Fig. 4.

-
- [1] C. M. Ho and Y. C. Tai, "Micro-electro-mechanical-systems(MEMS) and fluid flows," *Ann. Rev. Fluid Mech.* **30**, 579 (1998).
 - [2] E. Arkilic, K.S. Breuer, and M.A. Schmidt, "Gaseous slip flow in long micro-channels," *J. MEMS* **6**, 167 (1995).
 - [3] J. Koplik and J.R. Banvar, "Continuum deductions from molecular hydrodynamics," *Ann. Rev. Fluid mech.* **27**, 257 (1995).
 - [4] A. Beskok, G. E. Karniadakis and W. Trimmer, "Rarefaction and compressibility effects in gas micro-flows," *Journal of Fluids Engineering*, **118**, 448 (1996).
 - [5] Shiyi Chen and Gary D. Doolen, "Lattice Boltzmann method for fluid flows," *Ann. Rev. Fluid Mech.*, **30**, 329 (1998).
 - [6] S. Chen, H. Chen, D. Martinez, and W. H. Matthaeus, "Lattice Boltzmann model for the simulation of magneto-hydrodynamics," *Phys. Rev. Lett.* **67**, 3776 (1991).
 - [7] Y. H. Qian, D. d'Humières, and P. Lallemand, "Lattice BGK models for Navier-Stokes equation," *Europhysics Letters* **17**, 479 (1992).
 - [8] Shuling Hou, Qisu Zou, Shiyi Chen, Gary D. Doolen and Allen C. Cogley, "Simulation of incompressible Navier-Stokes fluid flows using a lattice Boltzmann method," *J. Comput. Phys.* **118**, 329 (1995).